Characterization of the Tryptophan Residues of Human Placental Ribonuclease Inhibitor and Its Complex with Bovine Pancreatic Ribonuclease A by Steady-State and Time-Resolved Emission Spectroscopy

Pinki Saha Sardar,[†] Shyam Sundar Maity,[†] Sanjib Ghosh,*[,†] Juin Chatterjee,[‡] Tushar Kanti Maiti,[‡] and Swagata Dasgupta[‡]

Department of Chemistry, Presidency College, Calcutta 700073, India, and Department of Chemistry, Indian Institute of Technology, Kharagpur 721302, India

Received: July 28, 2006

Human placental ribonuclease inhibitor (hRI) containing six tryptophan (Trp) residues located at positions 19, 261, 263, 318, 375, and 438 and its complex with RNase A have been studied using steady-state and time-resolved fluorescence (298 K) as well as low-temperature phosphorescence (77 K). Two Trp residues in wild-type hRI and also in the protein−protein complex with RNase A are resolved optically. The accessible surface area values of Trp residues in the wild-type hRI and its complex and consideration of inter-Trp energy transfer in the wild-type hRI reveal that one of the Trp residues is Trp19, which is located in a hydrophobic buried region. The other Trp residue is tentatively assigned as Trp375 based on experimental results on wild-type hRI and its complex. This residue in the wild-type hRI is more or less solvent exposed. Both the Trp residues are perturbed slightly on complex formation. Trp19 moves slightly toward a more hydrophobic region, and the environment of Trp375 becomes less solvent exposed. The complex formation also results in a more heterogeneous environment for both the optically resolved Trp residues.

Introduction

The protein of interest, the ribonuclease inhibitor (RI), is a 50 kDa protein present in the cytosol of mammalian cells that inhibits pancreatic-type ribonuclease. It is an acidic protein having a pI value of 4.7.[1] RI has been purified from human placenta by Blackburn et al.[2] It has also been isolated from pig liver and testis[3] as well as goat liver.[4] It is believed that RI serves to protect cellular RNA from degradation by engulfing pancreatic-type RNase that enters into the cytosol. In addition, RI regulates the biological activity of certain members of the ribonuclease family.[5]

Mammalian RIs contain 30−32 reduced cysteine residues. Oxidation of a single cysteine residue causes rapid oxidation of the remaining cysteine residues, which results in inactivation of RI.[6−7] Since RI also interacts with angiogenin, a blood-vessel-inducing protein with extraordinary affinity, and inhibits its ribonucleolytic as well as angiogenic properties, it is believed that it can be used for therapeutic purposes for cancers, tumors, and other diseases involving neovascularization.[8−10]

The structure of RI resembles a horseshoe. It consists of 15 leucine-rich, $\beta-\alpha$ repeat units arranged symmetrically in a semicircular manner.[11] The β-strands form a solvent-exposed β-sheet that forms the inner circumference of RI. The α-helices form the outer surface of the inhibitor. Human placental ribonuclease inhibitor (hRI) consists of 460 amino acids including six tryptophan (Trp) residues.[12] These are Trp19, Trp261, Trp263, Trp318, Trp375, and Trp 438. However, RI isolated from porcine liver (pRI) consists of 456 amino acids including five tryptophan residues.[13] These are Trp15, Trp257, Trp259, Trp314, and Trp 434. RI forms a 1:1 noncovalent complex with RNaseA and angiogenin and competitively inhibits their ribonucleolytic activities.[2,14−16] The dissociation constants of RI−RNase A and RI−Ang are in the fM range.[17] pRI and hRI bind RNase A almost identically.[14,16,18] Crystal structures have been determined for pRI with bovine pancreatic RNaseA[1] (PDB code 1DFJ) and hRI with human angiogenin[19] (PDB entry 1A4Y). Since the sequences of pRI and hRI are 85% similar and 77% identical, it can be assumed that similar contacts are present also in the hRI complex with RNase A. Again the overall docking of RNase A to RI resembles that of angiogenin.[11] It also has been shown that a tryptophan-rich area of hRI containing Trp261, Trp263, Trp318, and Trp375 plays an important role in the complex formed with RNaseA as well as with angiogenin.

Trp residues in proteins and complexes of proteins with other nonemissive molecules are often characterized by steady-state and time-resolved fluorescence of the Trp residue that acts as an intrinsic probe. However, interpretation of the results is not always unambiguous since the fluorescence spectra of Trp residues are always broad and the lifetime of fluorescence even in a protein containing a single Trp residue exhibits a multi-exponential decay. However, low-temperature phosphorescence (LTP) (77 K) spectra of Trp residues in proteins in a suitable cryosolvent always give structured spectra with definite (0,0) band characteristics of the Trp environment.[20−24] Several cases have also been reported where multi-tryptophan proteins give rise to more than one (0,0) band corresponding to different Trp residues indicating inefficient photoinduced energy transfer between Trp residues. The narrowness of the LTP bands, in contrast with the poorly resolved fluorescence of tryptophan, is attributed to the smaller excited-state dipole moment in the case of the triplet.[25] The LTP of the tryptophan residues buried

* Author to whom correspondence should be addressed. E-mail: sanjibg@cal2.vsnl.net.in.
[†] Presidency College.
[‡] Indian Institute of Technology.

10.1021/jp064832g CCC: $33.50
Published on Web 09/30/2006

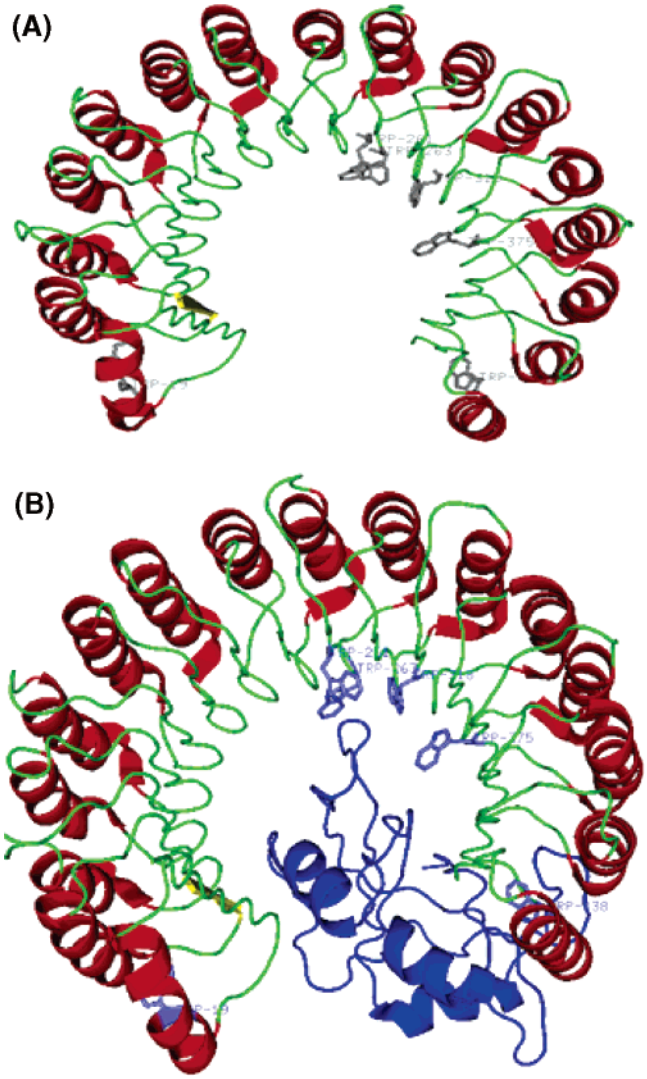

Figure 1. (A) Structure of hRI. Chain W of PDB code 1Z7X was rendered with PyMol (http://www.pymol.org). (B) Structure of hRI and its complex with bovine pancreatic RNase A. Chain X of PDB code 1Z7X was rendered with PyMol (http://www.pymol.org).

in hydrophobic regions within proteins is generally red-shifted relative to solvent-exposed residues, and it is better resolved since buried environments are usually more highly structured, i.e., homogeneous.[26] Specific interactions with polar residues, however, can result in blue-shifted origins for buried Trp residues.[27,28]

Low-temperature triplet state spectroscopy of biopolymers or biopolymer−substrate complexes in a proper cryosolvent often provides the same structural data as obtained by X-ray diffraction and NMR spectroscopy. Our earlier low-temperature triplet state studies of different mutants of T4 lysozyme molecules[21,29,30] showed that the spectral properties of the individual Trp residues are in complete agreement with their local environments as determined by X-ray crystallography.[31] Low-temperature triplet state studies of a mutated (Y45W) RNase T1 and its complexes with two ligands, the specific 2′-GMP and the 2′-AMP pseudosubstrates,[32] made in aqueous cryosolvent glass match very well with the crystallographic results.[33] There is complete agreement of the low-temperature triplet state studies[34] with the NMR studies of NCp7 binding with SL3[35] that Trp37 is in contact with G7 of the loop (2′) and that aromatic stacking is limited. It may be mentioned that a protein or protein−substrate complex in a proper cryosolvent upon cooling will seek lower-energy conformations on the potential energy landscape. Some of these will represent conformations of the systems at ambient temperatures, but the higher-energy representatives will not contribute at low temperature. This picture is also true in X-ray crystallographic structures where crystal packing forces restrict the number of conformations available in the natural environment.[36]

In this paper we characterize Trp residues of the wild-type hRI and the complex of hRI with RNase A by time-resolved fluorescence as well as low-temperature phosphorescence studies to provide meaningful results. We choose RNase A rather than angiogenin since it is devoid of any Trp residue.

The main objectives are to find out the

(i) environment of Trp residues in wild-type hRI and perturbation of the Trp environment due to binding with RNase A,

(ii) photophysical features of Trp residues in the wild-type hRI and its complex with RNase A, and

(iii) possibility of photoinduced energy transfer among Trp residues in wild-type hRI and its complex with RNase A.

The analysis of the data was carried out based on calculations using protein crystal structure data. Steady-state fluorescence data on the wild-type hRI and its several mutants W261A, W263A, W318A, 3W (W261A/ W263A/ W318A), and 4W (W261A/ W263A/ W318A/ W375A) carried out by Shapiro et al.[17] have also been utilized to interpret our results. The results will help understand the role of Trp residues in the Trp cluster region of hRI including Trp375 as well as the involvement of the two other Trp residues Trp19 and Trp438 in the binding process.

Experimental Methods

Materials. Human placental ribonuclease inhibitor (hRI) was from Bangalore Genei (India). Bovine pancreatic Ribonuclease A (RNase A) was from Sigma. All other chemicals from SRL (India) were of analytical grade. The purity of the protein was checked by sodium dodecyl sulfate polyacrylamide gel electrophoresis (SDS-PAGE). The complex was formed by incubating 165 μL of hRI (7.5 μM) with 35 μL of RNase A (107 μM) at 30 °C prior to recording of spectra. Glycerol used was of spectral grade (Aldrich).

Instrumentation. UV−vis absorption spectra were recorded on a Hitachi U-3210 spectrophotometer at 298 K. The steady-state fluorescence measurements at different excitations of 280, 285, 290, and 295 nm were made in a Hitachi F-4010 spectrofluorimeter (equipped with a 150 W xenon lamp) using a 1 cm path length quartz cuvette. All the measurements at 298 K were made by exciting the samples at 290 nm using 5 nm band-passes for excitation and emission using the correct mode of the instrument. Inner filter effects have been eliminated in all the emission spectra.

Emission studies at 77 K were made using a Dewar system having a 5 mm o.d. quartz tube. The freezing of the samples at 77 K was done at the same rate for all the samples. Triplet state emissions were measured in a Hitachi F-4010 spectrofluorimeter equipped with phosphorescence accessories at 77 K. All the samples were made in 40% glycerol for low-temperature measurements. The samples were excited at 280 nm using a 10 nm band-pass, and the emission band-pass was 1.5 nm. The cryosolvent (40% glycerol) used in the experiment was always found to form a clear glass. The low-temperature (77 K) spectra were found to be reproducible and free from any polarization artifacts. We have checked the low-temperature spectra using magic angle polarizer conditions (the excitation polarizer is

oriented in the vertical position and the emission polarizer is oriented 54.7° from the vertical) for standard samples such as bovine serum albumin (BSA) and horse liver alcohol dehydrogenase (HLAD).

Singlet state lifetime was measured by a Time Master fluorimeter from Photon Technology International (PTI). The system measures the fluorescence lifetime using PTI's patented strobe technique and gated detection. The software Felix 32 controls all acquisition modes and data analysis of the Time Master system. The sample was excited using a thyroton-gated nitrogen flash lamp (full width at half-maximum 1.2 ns) that is capable of measuring fluorescence time-resolved acquisition at a flash rate of 25 kHz. Lamp profiles were measured at the excitation wavelength (297 nm) using slits with a band-pass of 3 nm using Ludox as the scatterer. The decay parameters were recovered using a nonlinear iterative fitting procedure based on the Marquardt algorithm. The quality of fit has been assessed over the entire decay, including the rising edge, and tested with a plot of weighted residuals and other statistical parameters, e.g., the reduced χ^2 ratio and the Durbin−Watson (DW) parameters.

Method of Calculation of the Accessible Surface Area for the Wild-Type hRI and Its Complex with RNase A. The coordinates for the protein, hRI complexed with RNase A (1Z7X), have been downloaded from the Protein Data Bank.[37] There are two side chains for each protein: W and Y for RI and X and Z for RNase A. The coordinates of chain W were extracted from the file for calculations of the accessible surface area (ASA) for the uncomplexed form. The ASA has been calculated using the program NACCESS.[38] Default parameters were used for the calculations. Calculations for the complexed form were performed on chain W complexed with chain X.

Results and Discussion

Steady-State Fluorescence at 298 K. Using a hybrid quantum mechanical/classical molecular dynamics method Callis et al.[39] have emphasized that in proteins containing a single Trp residue fluorescence spectra are influenced by the effective electric field at the chromophore's site. This electric field can be largely determined by the charge distribution and the water of hydration on the protein surface. Another complication arises from the extent of spectral relaxation determined by the local mobility of the polypeptide.

In a protein containing more than one Trp residue, to use the intrinsic tryptophan luminescence as a probe for protein structure, function, and dynamics, one needs to find the spectral contributions of individual Trp residues.[40] The situation is often complicated if there is a nonradiative resonance energy transfer among the Trp residues having different microenvironments. Through the use of steady-state and time-resolved fluorescence it is really a challenge to assess the fluorescence contributions for an individual Trp residue in a protein when inter-Trp energy transfer takes place. The fluorescence of a protein containing multiple tryptophan residues should be the sum (or average) of the contributions from the various Trp emitting centers in the absence of inter-Trp energy transfer provided that none of the Trp residues are intrinsically quenched by a nearby residue.

Figure 2 shows the fluorescence spectra of the wild-type hRI and the complex of hRI with RNase A. Table 1 gives the position of λ_{max} and the intensity of the emission at λ_{max} for different excitation wavelengths. There is a small but gradual shift of the λ_{max} toward red as one changes the λ_{exc} from 280 to 295 nm for both wild-type and the complex under similar experimental conditions.

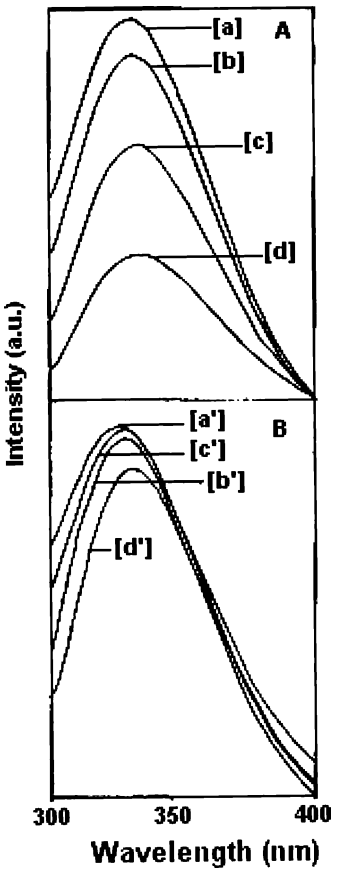

Figure 2. (A) Fluorescence spectra of the wild-type hRI at 298 K at different excitations: (a) $\lambda_{exc} = 280$ nm, (b) $\lambda_{exc} = 285$ nm, (c) $\lambda_{exc} = 290$ nm, (d) $\lambda_{exc} = 295$ nm. In each case the excitation and emission band-passes are 5 nm. The concentration of wild-type hRI is 7.5 μM. (B) Fluorescence spectra of the complex with RNase A at 298 K at different excitations: (a′) $\lambda_{exc} = 280$ nm, (b′) $\lambda_{exc} = 285$ nm, (c′) $\lambda_{exc} = 290$ nm, (d′) $\lambda_{exc} = 295$ nm. In each case the excitation and emission band-passes are 5 nm. The concentrations of wild-type hRI and RNase A are 7.5 and 107 μM, respectively.

TABLE 1: Fluorescence Data for Wild-Type hRI and Its Complex with RNase A at 298 K

sample	λ_{exc} (nm)	λ_{em}[a] (nm)	intensity at λ_{max}[b]
wild-type hRI	280	337.6	540.0
	285	338.0	496.1
	290	339.8	383.6
	295	340.6	236.0
hRI complex with RNase A	280	333.6	345.6
	285	335.0	345.3
	290	336.2	340.3
	295	338.0	199.2

[a] Errors in the measurements are ±0.4 nm. [b] The intensities are calculated in each case using the total area under the respective band.

Shapiro et al.[17] reported the fluorescence spectra at room temperature for wild-type hRI and several mutants: W261A, W263A, W318A, 3W (W261A/ W263A/W318A), and 4W (W261A/ W263A/W318A/W375A). Fluorescence spectra of the complex of hRI and its mutants with angiogenin were also reported. All mutations of Trp to Ala reduce the fluorescence intensity of the wild-type hRI. W261A induces the maximum loss of fluorescence (~30%). The Trp fluorescence emission of free 3W was ~50% lower than that of wild-type hRI. The Trp emission of free 4W was ~68% lower than that of wild-type hRI. It was also revealed that λ_{max} gradually shifts toward

the blue as one moves from W261A, to W263A, to W318A, to 3W, and to 4W.

The results of Shapiro et al.[17] imply that all the Trp residues in wild-type hRI are emitting and some of the Trps in the cluster are involved in inter-Trp energy transfer among themselves. The blue shift in case of 4W indicates that Trp19 and Trp438 reside in a hydrophobic buried environment compared to other Trp residues. Our results (Figure 2 and Table 1) also imply that Trp residues are in different environments and Trp19 is in a hydrophobic buried environment (see below). More importantly Trp residues in the complex are in a less solvent exposed environment compared to that in wild-type hRI (Figure 2 and Table 1).

Time-Resolved Studies at 298 K. The fluorescence decay of both wild-type hRI and the complex were monitored at 338 and 335 nm, respectively, under similar experimental conditions. The decays in both the cases were best fit by two components rather than three (Figure 3 and Table 2). Interpretations of complex decay of tryptophan fluorescence fall into two main categories: ground-state heterogeneity (e.g., rotamer model) and excited-state reaction (e.g., relaxation model). Proteins, in contrast, are heterogeneous systems with a hierarchy of internal motions that cover a wide range of correlation times, including the nanosecond time window of fluorescence. However, the excited-state reaction approach relies on protein dynamics to convert electronically excited indole into other spectroscopic species. More specifically, the relaxation model assumes that such a reaction involves reorientation of polar groups surrounding tryptophan in a protein.[41−43] Neither of the models has been unequivocally proven for any specific protein.

The two components at 3.9 and 0.4 ns (Table 2) indicate two different kinds of environments of emitting Trp in the wild-type hRI; the shorter one (<1 ns) usually arises from a blue-shifted emission of Trp in a comparatively buried region.[44] The lifetime of the complex also has two components at 4.5 and 0.6 ns (Table 2), with a somewhat larger contribution for the longer component. This definitely suggests that Trp residues in hRI are perturbed due to complex formation. The observation of the increased value of the shorter component (from 0.4 ns in the wild-type hRI to 0.6 ns in the complex) implies that Trp residues with a shorter-component lifetime in the wild-type hRI move to a different environment in the complex, which leads to reduced quantum yield of this class of Trp in the complex. Since hRI contains six Trp residues it is difficult to interpret the results in terms of a particular Trp residue. However, since four Trps reside in a cluster (all of these having more or less the same environment) it may be argued that one of these lifetimes is from the Trp residues in the cluster and the other is either Trp19 or Trp438 or both. (see next section)

Phosphorescence Spectra of the Wild-Type hRI and Its Complex with RNase A at 77 K. Figure 4 shows the phosphorescence spectra of the wild-type hRI and also its complex with RNase A in a 40% glycerol matrix at 77 K with λ_{exc} at 280 nm. The spectra of the wild-type hRI show two (0,0) bands located at 415.2 and 409.0 nm (Figure 4 and Table 3). The spectra of the complex also exhibit two (0,0) bands at 416.0 and 409.8 nm. The bandwidths (obtained by using a curve-fitting procedure) of both the (0,0) bands are given in Table 3.

Proteins containing more than one Trp residue generally exhibit a single (0,0) band in their phosphorescence spectra. The quenching may be due to

(i) energy transfer to another residue,

(ii) interaction with a neighboring residue, for instance, the formation of a charge-transfer complex, or

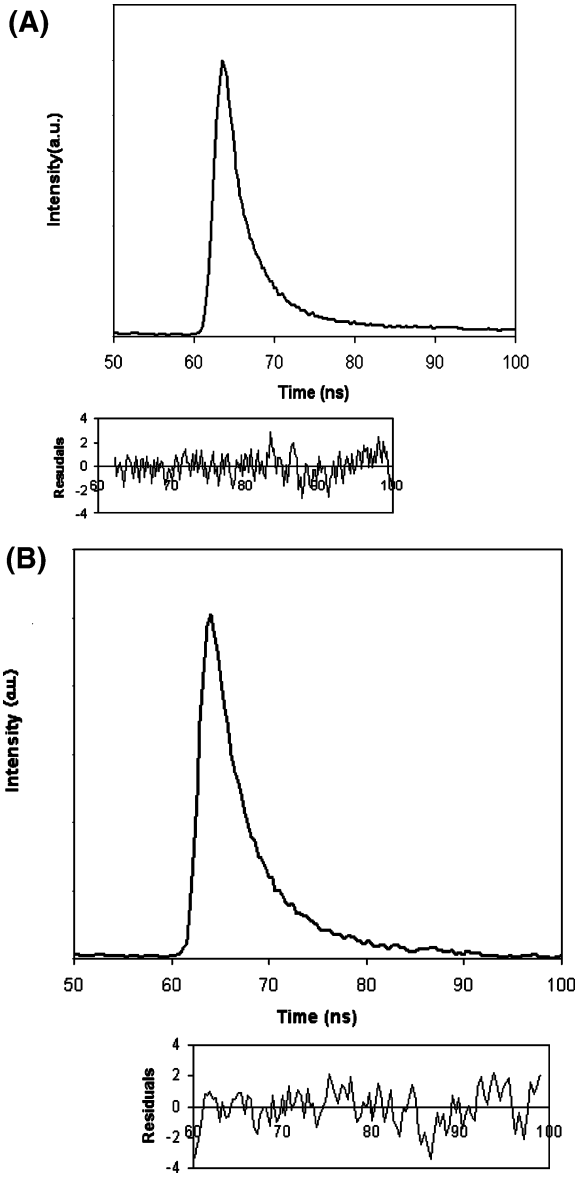

Figure 3. (A) Fluorescence decay curve of the wild-type hRI at 298 K. The excitation and emission wavelengths are 297 and 338 nm, respectively. The excitation and emission band-passes are 20 and 10 nm, respectively. The concentration of wild-type hRI is 7.5 μM. (B) Fluorescence decay curve of the complex with RNase A at 298 K. The concentrations of wild-type hRI and RNase A are 7.5 and 107 μM, respectively. The other parameters are the same as in part A.

TABLE 2: Fluorescence Lifetime Data for Wild-Type hRI and Its Complex with RNase A at 298 K

sample	λ_{exc} (nm)	$\lambda_{monitor}$ (nm)	lifetime τ (ns)	χ^2
wild-type hRI	297	338	3.9 (4.8%) 0.4 (95.2%)	1.11
hRI complex with RNase A	297	335	4.5 (11%) 0.6 (89%)	1.33

(iii) electron transfer from the excited state.

However, several proteins containing more than one Trp residue are known to exhibit multiple (0,0) bands[21−24,45,46] arising from different Trp residues. The observation of multiple (0,0) bands is usually possible when the Trp residues in a protein are in widely different environments and photoinduced energy transfer among the emitting Trp residues is prevented.

The energy transfer (ET) between two Trp residues in a protein could be due to singlet−singlet nonradiative energy

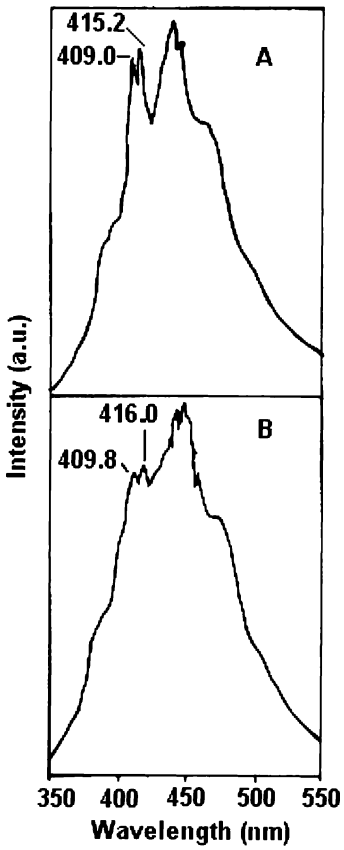

Figure 4. (A) Phosphorescence spectra of the wild-type hRI at 77 K: $\lambda_{exc} = 280$ nm. The excitation and emission band-passes are 10 and 1.5 nm, respectively. The concentration of wild-type hRI is 7.5 μM. (B) Phosphorescence spectra of the complex with RNase A at 77 K. The other parameters are the same as in part A.

TABLE 3: Phosphorescence Data for Wild-Type hRI and Its Complex at 77 K in a 40% Glycerol Matrix

sample	λ_{exc} (nm)	(0,0) band position[a] (nm)	width of the (0,0) band at half-maximum (cm^{-1})
wild-type hRI	280	409.0	180.0
		415.2	160.0
hRI complex with RNase A	280	409.8	215.0
		416.0	210.0

[a] Errors in the measurements are $\pm$0.2 nm

transfer by the dipole−dipole mechanism of Förster.[47] Triplet−triplet ET by Dexter's exchange mechanism[48] between two Trp residues is also possible if they are very close to each other (within 10 Å) and properly oriented with respect to each other.[24,49] Energy transfer over long distances (>10 Å) must occur by singlet−singlet nonradiative transfer following the Förster mechanism of dipole−dipole coupling.[47] The rate constants k^{tr}, in s^{-1}, for energy exchange between two species coupled by the Förster transfer mechanism[43] are given by

$$k^{tr} \cong (8.71 \times 10^{23})k^0 q r^{-6} \kappa^2 J n^{-4} \qquad (1)$$

In this equation, the donor has a decay constant, k^0, and radiative quantum yield q in the absence of energy transfer. Also, n is the refractive index of the medium between the donor and the acceptor, while J is an overlap integral between the donor luminescence and the acceptor absorption spectrum. The geometric variables in eq 1 are r, the distance between the centers of the donor and acceptor chromophores (in Å), and κ, the orientation factor for the dipole−dipole interaction. The factor κ^2 is given by

$$\kappa^2 = (\cos\theta - 3\cos\alpha\cos\beta)^2 \qquad (2)$$

where θ is the angle between the donor and the acceptor transition moments, and α and β are the angles made by the donor and acceptor transition moments, respectively, with the intermolecular vector.

TABLE 4: Inter-Trp Distances (in Å)[a]

Trp	261	263	318	375	438
19	37.02 (137)	37.66 (110)	38.83 (77)	37.29 (128)	39.00 (34)
261		6.96 (79)	6.07 (63)	12.59 (75)	30.15 (103)
263			10.37 (118)	14.60 (23)	29.70 (116)
318				7.56 (130)	25.96 (43)
375					18.48 (139)

[a] The angles between planes of the indole moieties in the tryptophan residues are given in parentheses.

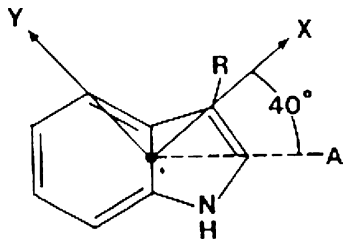

Figure 5. Indole moiety and transition dipole moment direction.

The hRI contains six Trp residues with four of them, Trp261, Trp263, Trp318, and Trp375, forming a cluster. In hRI the distance between Trp residues and their orientation with respect to each other (angle between indole planes) are given in Table 4. The long-wavelength absorption band of the tryptophan residue can be taken as a transition to the ^1L_a state.[50] Indole, however, is believed to have two closely spaced electronic states, which are ^1L_a and ^1L_b.[51] The relative energies of these two states are extremely sensitive to the nature of the solvent.[52] Several semiempirical calculations have suggested that the lowest electronic state of indole in the gas phase is the ^1L_b state, and the transition moment for this state has been calculated to lie anywhere between 25° and 88° from the *A*-axis (Figure 5) in the plane of the molecule.[53] Recent studies of the rotationally resolved electronic spectrum of indole in the gas phase[54] suggest that the transition moment lies $\pm(45° \pm 5°)$ with respect to the *A*-axis or roughly along either the *x*- or *y*-axis of Figure 5 . Taking the transition dipole moment of tryptophan as either the *x*- or the *y*-axis (Figure 5) and using the crystal structure data, we have calculated the geometric parameters (r and κ^2) among the different pairs of Trp residues. The likely candidates for triplet emission will be either

(i) one Trp from the cluster and Trp19,
(ii) one Trp from the cluster and Trp438, or
(iii) Trp19 and Trp438.

Two of the Trp residues in the cluster have much less probability of simultaneous emission because of efficient inter-Trp ET since they are close to each other and the orientation with respect to each other (Table 4) is favorable for ET.

The blue-shifted phosphorescence that is typical of free Trp in a polar solvent can be attributed to the lower polarizability of the environment and to the poor stabilization of the triplet state by a rigid solvation geometry that is organized to effectively stabilize the ground state by dipole−dipole alignment. The red-shifted (0,0) band is characteristic of a Trp residue located in a buried polarizable environment that stabilizes the triplet state more than the ground state.[28,32,46,55,56] Apart from solvent exposure, rigidity and immediate local charges also control the position of the (0,0) band.

The positions of the (0,0) bands in the wild-type hRI indicate that one of the Trp residues having a (0,0) band at 415 nm is buried in a hydrophobic environment and the other having a (0,0) band at 409 nm is partially exposed.

Our previous studies on lysozyme from bacteriophage T4 and its several mutants proved that the three tryptophan residues, Trp126, Trp138, and Trp158, exhibit phosphorescence (0,0) bands at 404.6, 413.6, and 407.7 nm, respectively.[21] The absolute value for the ASA in Å^2 (calculated using the protein coordinates taken from 2LYZ in the Protein Data Bank) are Trp126 = 48.45 Å^2, Trp138 = 12.72 Å^2, and Trp158 = 36.30 Å^2. Trp138 having the lowest ASA exhibits the most red-shifted phosphorescence (0,0) band while Trp126 having the largest ASA exhibits most blue-shifted phosphorescence (0,0) band. The correlation of the position of the phosphorescence (0,0) band and the ASA is well supported by the crystal structure data[31] where Trp138 is most buried, Trp126 is more or less exposed, and Trp158 is partially exposed.

In HLAD two distinct (0,0) bands of phosphorescence appear at 406.0 and 411.0 nm The (0,0) band at 411 nm corresponds to the buried Trp314 whereas the band at 406.0 nm is assigned to Trp15, which is more or less solvent exposed.[45,46] In our recent studies of *Escherichia coli* alkaline phosphatase (AP) (containing three Trp residues at 109, 220, and 268), its mutant W220Y and its Tb^{3+} complex (where two Zn^{2+} ions and one Mg^{2+} ion in wild-type protein are replaced by Tb^{3+}) reveal that Trp109 phosphorescence appears at 414.5 nm, and Trp220 at 411.4 nm. The ASA values of Trp109 are 0.68 Å^2 (in chain A) and 0.24 Å^2 (in chain B) whereas the ASA values of Trp220 are 59.92 Å^2 (in chain A) and 83.20 Å^2 (in chain B). Trp268 does not exhibit any phosphorescence band because of the proximity of the Cys^{286}−Cys^{336} disulfide bond revealed in the crystal structure of AP.[57] Disulfides are the only known intrinsic quenchers of Trp phosphorescence in proteins.[58] The bandwidth of the Trp109 (0,0) band is 40 cm^{-1}, the narrowest so far observed. This Trp109 is so far the most buried homogeneous residue[23] found in a protein. This is consistent with very small ASA values of Trp109 in both the chains. Optically detected magnetic resonance (ODMR) studies in AP[23] and T4 lysozyme[22,23] also support the correlation of the position of the (0,0) bands with solvent exposure.

Thus, in a given multi-Trp protein showing optically resolved (0,0) bands in their phosphorescence spectra, the positions of the (0,0) bands corresponding to different Trp residues correlate well with the solvent exposure of the Trp residues.

However, in the Trp repressor from *E. coli* (containing two Trp residues at positions 19 and 99) somewhat anomalous results were obtained.[59] Trp99 exhibits a red-shifted phosphorescence (0,0) band compared to that of Trp19. Although the phosphorescence and ODMR data for Trp99 are indicative of a typical interior residue, the fluorescence data show it to be relatively exposed to quenchers and solvent. These opposing results imply any or all of the following:[59]

(i) The environment of Trp99 stabilizes the excited triplet state, possibly due to the polarizability of groups around the indole ring.

(ii) There is a change in protein conformation upon freezing that occludes solvent molecules from the Trp99 local environment.

(iii) Local polar groups may be arranged such that the excited triplet state dipole of Trp99 is somewhat stabilized relative to the ground state.

An unusual environment of Trp 99 is suggested by the larger wavelength dependence of the zero field splitting (zfs) parameters (obtained by ODMR data in zero magnetic field) than is typically found for a residue buried in a polarizable microenvironment, e.g., Trp138 of T4 lysozyme.[21]

In the case of hRI both the (0,0) bands undergo only a very slight shift toward the red in the complex (Table 3). The assignment of the two (0,0) bands to particular Trp residues can be made based on the shift of the (0,0) band in the complex compared to that in the wild-type hRI (Table 3) and the change of the ASA on complex formation (Table 5). The ASA calculations for free hRI are performed on the structure of the complexed inhibitor after computational subtraction of the bound RNaseA. This is based on the assumption that there are no major structural rearrangements of the inhibitor during complex formation.

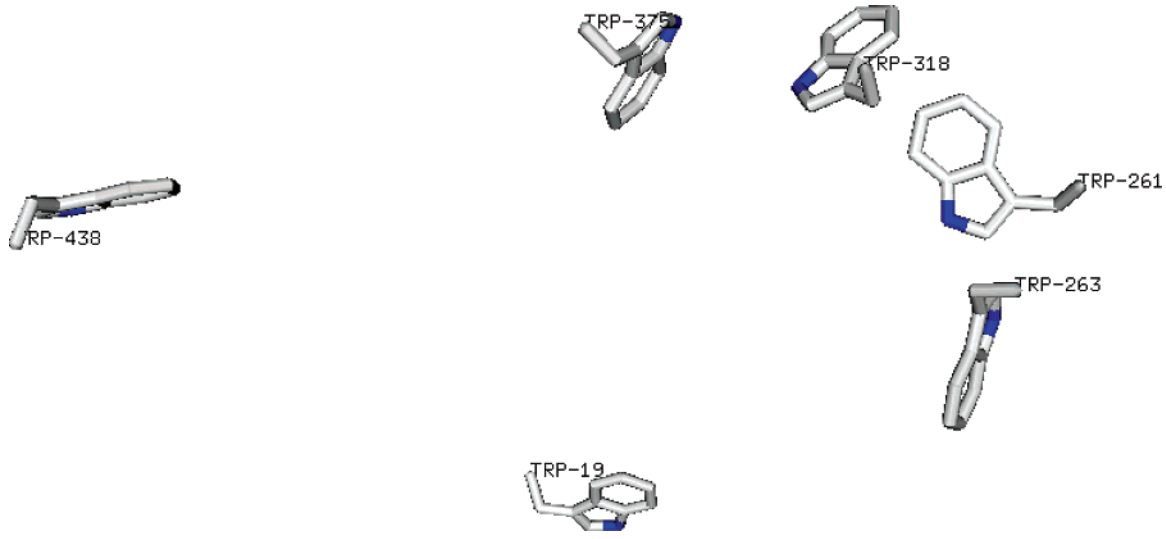

Figure 6. Orientations of six Trp residues with respect to each other in the wild-type hRI.

TABLE 5: Accessible Surface Areas (in Å²) for Each Trp Residue in Wild-Type hRI and Its Complex with RNase A for Chain W

residues	ASA for uncomplexed (Å²)	ASA for complexed (Å²)	% change in ASA
Trp19	7.97	7.97	0
Trp261	67.82	16.91	74
Trp263	66.92	21.82	66
Trp318	38.78	13.47	64
Trp375	86.28	42.04	51
Trp438	30.99	6.93	77.4

TABLE 6: Calculated Accessible Surface Areas (in Å²) of Free pRI and pRI Chain I Extracted from the Complex of pRI and RNase A

sample	residues	ASA (Å²)	total ASA (Å²)[a]
free pRI	Trp15	20.01	
	Trp257	54.64	18 656.8
	Trp259	63.79	(absolute sums over
	Trp314	79.57	all chains)
	Trp434	48.42	
pRI extracted	Trp15	13.58	
from the complex	Trp257	46.57	18 797.4
	Trp259	53.13	(chain I extracted from
	Trp314	76.46	the complex, absolute
	Trp434	30.60	sums over all chains)

[a] The difference in total ASAs for the free form and extracted chain I is 140.6 Å² (0.75%).

Although the crystal structure of free hRI is not known yet, the crystal structures of both the free pRI (porcine ribonuclease inhibitor containing five tryptophan residues)[1] and its complex with RNase A[11] are known. Thus one can compare the ASA values of Trp residues in the free pRI with the ASA values of Trp residues obtained by computational subtraction of the bound RNase A from the complex of pRI and RNase A. (This method is used for the calculation of the ASAs of Trp residues in the free hRI.) We calculated the values of ASA for pRI and found that:

(i) There is a similar trend for the ASA values of five Trp residues in the free pRI and in the pRI extracted from the pRI−RNase A complex. (Table 6)

(ii) There is only a minor change (0.75%) in the total ASA in the free pRI from the values obtained by the subtraction procedure (Table 6).

Since the binding constants of the hRI and the pRI with RNase A are of similar magnitudes[17,14] and since there is a high percentage of homology between the hRI and the pRI,[14,16−18] it may be presumed that there are no major structural rearrangements of the tertiary structure of the inhibitor hRI during complex formation. Thus one can safely assume that the results obtained by the computational subtraction procedure used to calculate the ASA of the Trp residues in the hRI practically resemble those in the free hRI.

Since all the Trp residues except Trp19 undergo a considerable change of the ASA (Table 5) on complex formation, the 415.2 nm band is assigned to Trp19. The (0,0) band position of 415.2 nm is also correlated well with the ASA value of Trp 19, the ASA value being the least among all of the Trp residues in the wild-type. This interpretation also supports the work of Shapiro et al.[17] where the 4W mutant of hRI (containing Trp19 and Trp438) shows blue-shifted fluorescence compared to wild-type hRI and other mutants.

It is difficult to assign any particular Trp residue corresponding to the (0,0) band around 409 nm. However, one can eliminate Trp438 since after complex formation Trp438 has the lowest ASA among all of the Trp residues. The slight red shift of both the (0,0) bands in the complex support this contention. Thus the 409 nm band should arise from one of the Trp residues in the cluster. We tentatively assign the 409 nm band to Trp375 for the following reasons:

(i) Trp375 undergoes the least change in the ASA on complex formation (Table 5).

(ii) ASA of Trp 375 in the wild-type is 86.28 Å², which implies that it is more or less exposed; ASA of Trp375 in the complex (42.04 Å²) is less exposed to solvent and is consistent with the red shift of the (0,0) band.

We also present a list of tryptophan neighbors within 6 Å from the nitrogen (NE1) of the indole moiety of Trp in Table 7. The nearest polar residue for each Trp is also indicated. Thus it appears that the ASA is the more dominating factor than the effect of immediate local charges arising from the polar residue surrounding each Trp in wild-type hRI in determining the position of the (0,0) band of the phosphorescence spectra.

The above interpretation is corroborated by the results of time-resolved studies mentioned in the earlier section. The width of the phosphorescence (0,0) band reflects the heterogeneity of the Trp environment[23] in a protein. The most homogeneous environment so far observed in a protein is for Trp109 in AP from *E. coli*.[23] Trp109 in AP exhibits a bandwidth of 40 cm^{-1}.[23] In this case Trp19 of the wild-type hRI is in a more homogeneous environment than the Trp residue corresponding

TABLE 7: Tryptophan Neighbors within 6 Å[a]

TRP 19	TRP 261	TRP 263	TRP 318	TRP 375	TRP 438
LEU 14	GLU 206	GLU 206 (2.72 Å)	TRP 261	TRP 318	LEU 409
SER 15	GLU 230	SER 207	LYS 286	GLU 344 (2.63 Å)	GLY 410
ASP 16	LEU 231	ALA 232	GLU 287	LEU 345	ASP 411
ALA 17	ALA 232	LEU 233	LEU 288	GLN 346	ILE 414
ARG 18	LEU 233	GLY 234	SER 289	ILE 347	LEU 433
ALA 20	GLY 234	SER 235	LEU 290	SER 348	TYR 434
GLU 21	THR 259	ASN 236	ALA 291	VAL 373	ILE 436
LEU 22	LEU 260	TRP 261	SER 316	LEU 374	TYR 437
PRO 24	ILE 262	ILE 262	LEU 317	LEU 376	SER 439
LEU 26	TRP 263	GLU 264	VAL 319	ALA 377	GLU 440
LEU 34	CYS 265	CYS 265	LYS 320	CYS 379	MET 442
LEU 39	GLU 287	GLY 266	CYS 322	GLU 401	GLU 443 (2.68 Å)
ALA 42	LEU 288	SER 289	GLU 344	LEU 402	LEU 446
ARG 43	SER 289	LEU 290	LEU 345	ASP 403	VAL 458
CYS 44	TRP 318	ALA 291	GLN 346	VAL 432	ILE 459
ASP 46 (2.72 Å)[b]		GLY 292	ILE 347		SER 460
ILE 47		ASN 293	TRP 375		

[a] Distances are from the nitrogen (NE1) of the indole moiety of Trp. [b] The distance mentioned here is the nearest position of the polar residues from the Trp residues.

to the (0,0) band at 409.0 nm (Table 3). It is interesting to note that both the Trp residues in the complex have larger widths of the (0,0) bands compared to those in wild-type hRI. This indicates that Trp residues in the complex move to a more heterogeneous environment than that in the wild-type hRI.

Conclusions

Photophysical studies of the wild-type hRI and its complex with RNase A using steady-state and time-resolved fluorescence and phosphorescence at 77 K reveal the following:

(i) Two different types of environments of emitting Trp residues are observed from both time-resolved fluorescence and low-temperature phosphorescence.

(ii) The ASA value remains the same for Trp19 upon complex formation whereas other Trp residues undergo changes in ASA ranging from 50% to 77%.

(iii) The experimental results, ASA calculations, and consideration of inter-Trp ET suggest that Trp19 is emitting and situated in a buried hydrophobic environment in wild-type hRI and undergoes a slight change in environment (slightly more hydrophobic) in the complex. The homogeneity of the Trp19 environment is, however, less in the complex than that in the wild-type.

The other emitting Trp is argued to be Trp375 in the Trp cluster region of hRI. The experimental results directly suggest that Trp375 is less exposed in the complex compared to the wild-type protein. The study of the protein−protein complex presented here is a unique attempt to identify the optically resolved Trp residues by exploiting luminescence spectroscopic data and several calculations using the crystal structures of the protein and protein complex.

Acknowledgment. This work was funded by the Department of Science and Technology, Government of India (Grant Nos. SR/S1/PC/34-02 and SR/S5/NM/14-2003) for funding and junior research fellowships. We acknowledge the reviewer for his valuable suggestions.

References and Notes

(1) Kobe, B.; Deisenhofer, J. *J. Mol. Biol.* **1996**, *264*, 1028−1043.
(2) Blackburn, P.; Wilson, G.; Moore, S. *J. Biol. Chem.* **1977,**. *252*, 5904−5910.
(3) Ferreras, M.; Gavilanes, J. G.; Lopez-Otin, C.; Garcia- Segura, J. M. *J. Biol. Chem.* **1995**, *270*, 28570−28578.
(4) Chatterjee, J.; Maiti, T. K.; Dasgupta S. *Protein Pept. Lett.* **2006**, *13*, 779−783.
(5) Shapiro, R.; Vallee, B. L. *Proc. Natl. Acad. Sci. U.S.A.* **1987**, *84*, 2238−2241.
(6) Blázquez, M.; Fominaya, J. M.; Hofsteenge, J. *J. Biol. Chem.* **1996**, *271*, 18638−18642.
(7) Kim, B. M.; Schultz, L. W.; Raines, R. T. *Protein Sci.* **1999**, *8*, 430−434.
(8) Nobile, V.; Russo, N.; Riordan, J. F. *Biochemistry* **1998**, *37*, 6857−6863.
(9) Fett, J. W.; Olson, K. A.; Rybak, S. M. *Biochemistry* **1994,** *33*, 5421−5427.
(10) Olson, K. A.; French, T. C.; Vallee, B. L.; Fett, J. W. *Cancer Res.* **1994**, *54*, 4576−4579.
(11) Kobe, B.; Deisenhofer, J. *Nature* **1993**, *366*, 751−756.
(12) Lee, F. S.; Fox, E. A.; Zhou, H.-M.; Strydom, D. J.; Vallee, B. L. *Biochemistry* **1988**, *27*, 8545−8553.
(13) Hofsteenge, J.; Kiefer, B.; Matthies, B. A.; Stone, S. R. *Biochemistry* **1988**, *27*, 8537−8544.
(14) Dickson, K. A.; Haigis, M. C.; Raina, R. T. *Prog. Nucleic Acids Res. Mol. Biol.* **2005**, *80*, 349−374.
(15) Hofsteenge, J. In *Ribonucleases: Structures and Functions*; D'Alessio, G., Riordan, J. F., Eds.; Academic Press: New York, 1997; pp 621−658.
(16) Lee, F. S.; Shapiro, R.; Vallee, B. L. *Biochemistry* **1989**, *28*, 225−230.
(17) Shapiro, R.; Ruiz-Gutierrez, M.; Chen, C. Z. *J. Mol. Biol.* **2000**, *302*, 497−519.
(18) Vicentini, A. M.; Keifer, B.; Matthies, R.; Meyhack, B.; Hemmings, B. A.; Stone, S. R.; Hofsteenge, J. *Biochemistry* **1990,** 29, 8827−8834.
(19) Papageorgiou, A. C.; Shapiro, R.; Acharya, K. R. *EMBO J.* **1997**, *16*, 5162−5177.
(20) Maki, A. H. In *Biological Magnetic Resonance*; Berliner. L. J., Reuben J., Eds.; Plenum Press: New York, 1984; Vol. 6, pp 187−294.
(21) Ghosh, S.; Zang, L.-H.; Maki, A. H. *J. Chem. Phys* **1988**, *88*, 2769−2775.
(22) Ghosh, S.; Zang, L.-H.; Maki, A. H. *Biochemistry* **1988,** *27*, 7816−7820.
(23) Ghosh, S.; Misra, A, Ozarowski, A.; Stuart, C.; Maki, A. H. *Biochemistry* **2001,** *40*, 15024−15030.
(24) Ghosh, S.; Misra, A, Ozarowski, A.; Maki, A. H. *J. Phys Chem. B* **2003**, *107*, 11520−11526.
(25) Hahn, D. K.; Callis, P. R. *J. Phys. Chem. A* **1997**, *101*, 2686−2691.
(26) Galley, W. C.; Purkey, R. M. *Proc. Natl. Acad. Sci. U.S.A.* **1970**. *67*, 1116−1121.
(27) Hershberger, M. V.; Maki, A. H.; Galley, W. C. *Biochemistry* **1980,** *37*, 2204−2209.
(28) Ozarowski, A.; Barry, J. K.; Matthews, K. S.; Maki, A. H. *Biochemistry* **1999,** *38*, 6715−6722.
(29) Zang, L.-H, Ghosh, S.; Maki, A. H. *Biochemistry* **1989**, *28*, 2245−2251.
(30) Zang, L.-H.; Ghosh, S.; Maki, A. H. *Biochemistry* **1988**, *27*, 7816−7820.
(31) Remington, S. J.; Anderson, W. F.; Owen, J.; Ten Eyck, L. F.; Grainger, C. T.; Matthews, B. W**.** *J. Mol. Biol.* **1978**, *118*, 81−98.
(32) Lam, W. C.; Maki, A. H.; Itoh, T.; Hakoshima, T. *Biochemistry* **1992**, *31*, 6756−6760.
(33) Hakoshima, T.; Itoh, T.; Tomita, K.i.; Gohda, K.; Nishikawa, S.; Morioka, H.; Uesugi, W.i.; Ohtsuka, E.; Ikehara, M. *J. Mol. Biol.* **1992**, *223*, 1013−1028.
(34) Wu. J. Q.; Ozarowski, A.; Maki, A. H.; Urbaneja, M. A.; Henderson, L. E.; Casas-Finet, J. R. *Biochemistry* **1992**, *36*, 12506−12518.
(35) De Guzman, R. N.; Wu, Z. R.; Stalling, C. C.; Pappalardo, L.; Borer, P. N.; Summers, M. F. *Science* **1998**, *279*, 384−388.
(36) Maki, A. H. Professor Emeritus, Department of Chemistry, University of California at Davis, Davis, CA. Private communication.
(37) Berman, H. M.; Westbrook, J.; Feng, Z.; Gilliland, G.; Bhat, T. N.; Shindyalov, I. N.; Bourne, P. E**.** The Protein Data Bank. *Nucleic Acids Res.* **2000**, *28*, 235−242.
(38) Hubbard, S. J.; Thornton, J. M. *NACCESS, Computer Program*; Department of Biochemistry and Molecular Biology, University College London: London, 1993.
(39) Vivian, J. T.; Callis P. R. *Biophys. J.* **2001**, *80*, 2093−2109.
(40) Royer, C. A.; Gardner, J. A.; Beechem, J. M.; Brochon, J. C.; Matthews, K. S. *Biophys. J.* **1990** *58*, 363−378.
(41) Lakowicz, J. R.; Cherek, H. *J. Biol. Chem.* **1981**, *256*, 6348−6353.
(42) Lakowicz, J. R.; Balter, A. *Photochem. Photobiol.* **1982**, *36*, 125−132.
(43) Lakowicz, J. R.; Balter, A. *Biophys. Chem.* **1982**, *15*, 353−360.
(44) Szabo, A. G.; Rayner, D. M. *J. Am. Chem. Soc.* **1980**, *102*, 554−563.
(45) Eftink, M. R. In *Advances in Biophysical Chemistry*; Bush, C. A., Ed.; JAI Press: Greenwich, CT, 1992; Vol.2, pp 81−114.
(46) Purkey, R. M.; Galley, W. C. *Biochemistry* **1970**, *9*, 3569−3575.
(47) (a) Förster, T. Zwischenmolekulare energiewanderung und fluoreszenz. *Ann. Phys. (Leipzig)* **1948**, *2*, 55−75. (b) Förster, T. *Discuss. Faraday. Soc.* **1959**, *27*, 7−17.
(48) Dexter, D. L. A theory of sensitized luminescence in solids. *J. Chem. Phys.* **1953**, *21*, 836−850.
(49) Schlyer, B. D.; Steel, D. G.; Gafni, A. *J. Biol. Chem.* **1995**, *270*, 22890−22894.
(50) Weber G. *Biochem. J.* **1960**, *75*, 335−345.
(51) Song, P. S.; Kurtin, W. E. *J. Am. Chem. Soc.* **1969**, *91*, 4892−4906.
(52) (a) Strickland E. H.; Billups, C. *Biopolymers* **1973**, *12*, 1989−1995. (b) Tatischeff, I.; Klein, R.; Zemb, T.; Duquesne, M. *Chem. Phys. Lett.* **1978**, *54*, 394−398.
(53) Yamamoto, Y.; Tanaka, J. *Bull. Chem. Soc. Jpn.* **1972**, *45*, 1362−1366.
(54) Philips, L. A.; Levy, D. H. *J. Chem. Phys.* **1986**, *85*, 1327.
(55) Von Shutz, J. U.; Zuclich, J. A.; Maki, A. H. *J. Am. Chem. Soc.* **1974**, *96*, 714−718.
(56) Kwiram, A. L.; Ross, J. B. A. *Annu. Rev. Biophys. Bioeng.* **1982**, *11*, 223−249.
(57) Stee, B.; Holtz, K. M.; Kantrowitz, E. R. *J. Mol. Biol.* **2000**, *299*, 1303−1311.
(58) Li, Z.; Galley, W. C. *Biophys. J.* **1989**, *56*, 353−360.
(59) Eftink, M. R.; Ramsay, G. D.; Burns, L.; Maki, A. H.; Mann, C. J.; Matthews, C. R.; Ghiron, C. A. *Biochemistry* **1993**, *32*, 9189−9198.